Scientific African 19 (2023) e01471

Contents lists available at ScienceDirect

Scientific African

journal homepage: www.elsevier.com/locate/sciaf

Chemometrics validation of adsorption process economy: Case study of acetaminophen removal onto quail eggshell adsorbents

Adejumoke A. Inyinbor[a,f,*], Deborah T. Bankole[a,f], Folahan A. Adekola[b], Olugbenga S. Bello[c], Toyin Oreofe[d], Kelvin Amone[a], Adewale F. Lukman[e]

[a] Department of Physical Sciences, Landmark University, P.M.B 1001, Omu Aran, Nigeria
[b] Department of Industrial Chemistry, University of Ilorin, P.M.B 1515, Ilorin, Nigeria
[c] Department of Pure and Applied Chemistry, Faculty of Sciences, Ladoke Akintola University of Technology, P.M.B. 4000, Ogbomoso, Nigeria
[d] Department of Chemical Engineering, College of Engineering, Landmark University, P.M.B 1001, Omu Aran, Nigeria
[e] Department of Epidemiology and Bio-Statistics, University of Medical Sciences, Nigeria
[f] Landmark University Clean water and Sanitation Sustainable Development Goal, Landmark University, P.M.B 1001, Omu Aran, Nigeria

ARTICLE INFO

Article history:
Received 3 July 2022
Revised 24 November 2022
Accepted 24 November 2022

Editor: DR B Gyampoh

Keywords:
Acetaminophen
Adsorption
OLS
Eggshell

ABSTRACT

The potential of quail eggshells for acetaminophen (PCM) removal in aqueous solution was studied. Calcination greatly increased the surface area of the raw quail eggshell (RQES). Hence, surface area as determined by the Brunauer-Emmet-Teller (BET) surface and porosity analyzer are 680.80 m^2/g for RQES while calcinated quail eggshell (CQES) had 927.30 m^2/g. The scanning electron microscopic (SEM) analysis revealed pores useful for uptake of PCM. Adsorption process for the uptake of PCM onto RQES and CQES was pH-dependent with optimum pH of 7 and 6 respectively. The Freundlich adsorption isotherms suggested a multilayer adsorption of PCM unto RQES and CQES. The Dubinin Raduskevich (D-R) model best described the adsorption processes. The energy of adsorption obtained from the model for the two adsorption systems were 23.57 and 8.4515 kJ.mol^{-1} suggesting that chemisorption occurred within the systems. The maximum monolayer adsorption capacities were 10.00 and 15.15 mg/g for uptake of PCM unto RQES and CQES respectively. Pseudo-second-order model best explained the kinetics of the adsorption processes, adsorption process was established to be feasible and feasibility increased with temperature. The process economy validation by Ordinary Least Square (OLS) cum ridge estimator followed by model performance judgment using the test mean squared error (TMSE) revealed 32% and 22.8% in PCM quantity adsorbed per unit changes in time and temperature respectively. Hence, a valid justification for economy friendliness of the prepared adsorbents in acetaminophen removal.

* Corresponding author.
E-mail address: inyinbor.adejumoke@landmarkuniversity.edu.ng (A.A. Inyinbor).

https://doi.org/10.1016/j.sciaf.2022.e01471

Introduction

The importance of pharmaceuticals to the world's population cannot be overemphasized. Pharmaceuticals help to alleviate different types of infections and diseases in human and animals. Subsequently improving the quality of health and life expectancy [1]. Acetaminophen (PCM) is a pain-relieving, antipyretic analgesic, which is one of the most frequently consumed first-line drug all over the world [2]. Frequent detection of PCM molecules in water has been reported [3]. The discharge route for PCM into water bodies include the release of industrial effluents, improper disposal of hospital wastes and, egestion from man via urine. Up to 68% of the dosage being consumed is released into accessible water bodies through urine [4,5].

Concentrations of PCM in effluents and surface water have been greatly reported to exceed the expected limits [2,6]. High level of PCM was detected in Jakarta Bay water by Koagouw crew, who concluded that the analyzed concentration level calls for concern [7]. Varying PCM concentrations have also been reported in different kinds of water in some European countries [5,8]. These pharmaceuticals have biological activity [9] and accumulative tendency in aquatic organisms. PCM degraded product (4-aminophenol) is highly toxic and carcinogenic [4]. Unmetabolized PCM has also been reported to inhibit DNA synthesis leading to chromosomal aberrations [5,10]. PCM is therefore considered a contaminant that should be removed from effluents before discharging into the environment.

Several methods of pharmaceutical residue removal have been employed, which are accompanied by multiple challenges. Some of such methods include, advanced oxidation process, which requires large quantity of reagents for the operation [11]. The membrane filtration process with characteristics high cost and membrane stench over time [12]. The electrocoagulation process requires regular electrode replacement thus accumulates cost [13]. However, adsorption has found a wide application because of its low operational cost, simplicity and, efficiency [14–16,18,21]. The use of agricultural wastes and other waste materials have gained attention due to its low cost, availability and effectiveness. This practice has helped to combat the high-cost limitation of commercial activated carbon. Adsorption can be used for pollutants removal even at trace levels [21]. Activated carbon is porous, with a surface area presenting an exceptional adsorption capacity. Activated carbon has been prepared by exploring various waste biomass with excellent quality and characteristics [4]. Some of such biomass include castor oil seeds [22], eggshells [23], orange peels [2], kola-nut husks [24], snail shells [25], rice husk [26], cotton stalk [27] and, avocado seed [28] amongst others.

Numerous report exists on the use of lignocellulosic materials in adsorption studies, however, the use of protein-based waste as alternative adsorbent has been scarcely reported [29]. Protein-based material such as the quail eggshells satisfies the query of abundance. Since the introduction of the Japanese quail into Nigeria system in 1992, quail has become a major domestic and commercial livestock [30]. Hence, the quail eggshell is one protein based material that may serve as a good adsorbent. Proteins-based materials usually possess functional groups carrying heteroatoms (S, N and, O) which could present a good surface for complexation and bonding with pollutants. For instance, the membrane of eggshell is known to possess the thiol (-SH), amino ($-NH_2$), carbonyl (C = O), carboxyl (-COOH) and, hydroxyl (-OH) groups amongst others [31]. These functional groups would make the membrane of eggshell highly effective for various pollutant uptake. In addition, eggshells are known to have catalytic degradation characteristics [32]. The membrane of chicken eggshell and its whole eggshell matrix have been previously reported for the uptake of some organic pollutants [23,31–34]. However, to the best of our knowledge, reports focusing on utilizing the quail eggshell membrane and its whole eggshell matrix in the uptake of pharmaceutical pollutants are scarce; hence the novelty of this study.

We herein maximized quail eggshells waste for the adsorption of acetaminophen from aqueous media. The prepared raw quail eggshell (RQES) and calcined quail eggshell (CQES) were fully characterized. Various adsorption operational parameters were studied to validate the applicability of the prepared adsorbents. Kinetics, isotherms and, thermodynamics were employed to establish the mechanism and feasibility of the adsorption process. In addition, researchers have continued to justify the economic advantage of adsorption process based on the use of low-cost adsorbent thus neglecting the cost implication of the adsorption process. Hence, we herein for the first time employed the Ordinary Least Square (OLS) to justify and validate adsorption process economy in acetaminophen uptake unto quail eggshells.

Materials and methods

Materials collection and pretreatment

Quail eggshells were received as a kind gesture from the Teaching and Research Farm, of Landmark University, Omu Aran, Kwara State, Nigeria. The shells were thoroughly washed using deionized water and dried at 105 °C for 4 h to eradicate the moisture and finally powdered as well as screened through a particle size of 150 – 250 µm. Powdered sample (RQES) were divided into two; while a portion was stored for use, the second portion was further treated via calcination at 600 °C for 4 h. The resulting adsorbent (CQES) was also stored for use in adsorption studies.

Preparation of PCM solution

A 200 mg/L solution of PCM was prepared in a 1-liter standard flask using a 200 mg mass of pure PCM active received as a gracious donation from Tuyil Pharmaceuticals, Ilorin. All other working solutions were prepared by serial dilutions. The structure of PCM is presented in Fig. 1.

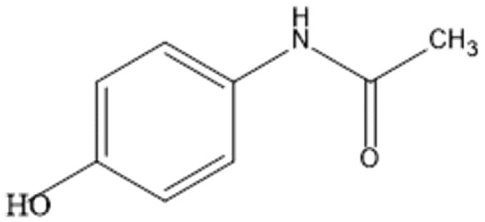

Fig. 1. Structure of Paracetamol molecule.

Characterization of RQES and CQES

The morphological character, surface chemistry, surface area and, elemental analysis may provide a better understanding of the adsorbate-adsorbent interactions. The morphological features and elemental composition were determined using a FEIESEM Quanta 200 for Scanning Electron Microscopy (SEM) and Energy Dispersive Xray (EDX). The average pore diameter and Brunauer Emmett Teller (BET) surface area were analyzed with a Micrometrics Tristar II surface area analyzer. The functional groups present in the prepared samples were detected using Bruker Alpha Fourier Transform Infrared spectrometer. The pHpzc of the prepared adsorbents was obtained using an established method [19].

Adsorption studies on RQES and CQES

The efficiencies of RQES and CQES adsorbents for the adsorption of PCM were investigated. Parameters influencing the nature and behavior of adsorbate as well as the surface charge on the adsorbent in solution were studied. These parameters include Initial solution pH (2–10), contact time (240 min) and initial adsorbate concentration (3, 6 and 10 ppm), adsorption system temperature (30, 40, 50 and 60 °C) and, adsorbent dosage (1–8 g/L). The amount of unadsorbed PCM at a given time q_t (mg/g) was calculated using Eq. (1).

$$q_{t=\frac{(C_i-C_t)}{M}\ x\ V} \tag{1}$$

Ci and *Ct* are defined as the mg/L concentrations of PCM solution at initial and at time *t*, *V* and M are the adsorbate volume in liters and adsorbent mass in grams respectively [19].

Isotherm studies

0.1 g of RQES and CQES each was added to 100 cm^3 of 100 ppm PCM solution. The mixture was agitated at 130 rpm on a mechanical shaker for 240 min. An optimal pH of 6 and 7 were used for CQES and RQES respectively. These conditions were used to obtain the equilibrium, kinetics and thermodynamics data with variation of parameters in specific studies. Equilibrium data were subjected to Langmuir, Freundlich, Dubinin-Radushkevich and, Temkin models. Various calculated isotherm parameter may provide information depicting many surface properties of the adsorbent cum adsorbent-adsorbent interaction. Hence, a vivid picture of the mechanism of adsorption. Table 1 highlights the Isotherms used in this work and their corresponding important parameters. The favourability of the adsorption process can be justified by the dimensionless parameter R_L, this can be calculated using equation

$$R_L = \frac{1}{(1 + K_L C_o)} \tag{2}$$

Kinetic models

The mechanism of adsorption process may be well understood via kinetic modeling of adsorption data. Here, The data from the kinetics study was fitted to the pseudo-first-order, pseudo-second-order, Elovich and intraparticle diffusion models. Table 2 highlights the important information for the mentioned kinetics models.

Thermodynamic studies

The feasibility, randomness and spontaneity of PCM adsorption unto RQES and CQES were studied Eqn (3) and (4).

$$lnK_0 = \frac{\Delta S^o}{R} - \frac{\Delta H^o}{RT} \tag{3}$$

$$\Delta G^o = -RT\,lnK_o \tag{4}$$

T which is the temperature has its dimension in K, K_o, is usually obtained from quantity adsorbed and concentration at equilibrium, and R is the gas constant. The values of ΔS^o *and* ΔH^ocan be gotten from the plot of K_o *versus* $\frac{1}{T}$.

Table 1
Isotherms used and their corresponding important parameters.

Isotherm	Linear equation	Plot	Important parameter	Reference
Langmuir	$\frac{C_e}{q_e} = \frac{C_e}{q_{max}} + \frac{1}{q_{max}K_l}$	$\frac{C_e}{q_e}$ *vs* C_e	Q_{max}, K_L, R_L	[35]
Freundlich	$\log q_e = \frac{1}{n} logC_e + logK_f$	$log\ q_e$ vs $logC_e$	k_f, n	[36]
Dubinin-Radushkevich	$lnq_e = lnq_o - \beta\varepsilon^2$ $\varepsilon = RTln\left(1 + \frac{1}{C_e}\right)$ $E = \sqrt{\frac{1}{2\beta}}$	lnq_e *vs* ε^2	q_o, β	[37]
Temkin	$q_e = BlnA + BlnC_e$ $B = {}^{RT}/_{b}$	q_e vs lnC_e	A_T, b_T	[38]

q_e and C_e are the equilibrium adsorptive capacity of the adsorbent and adsorbate equilibrium concentration respectively in (mg/L). K_L (L/mg) is the Langmuir constant; q_{max} (mg/g) is the maximum monolayer adsorption capacity; these parameters are usually calculated from the slope and the intercept of the plot C_e/q_e versus C_e. K_L is an important parameter in calculating R_L which is dimensionless and explains the favorability of the adsorption process. n and K_f (mg/g) are Freundlich constants that integrate the factors affecting adsorption intensity and capacity respectively. T (K) is the temperature, R (J/mol/K) is the gas constant, β (mol^2/kj^2) and q_o (mg/g) can be calculated from the slope and intercept of the plot of q_e *vs* ε^2. Temkin isotherm assumes linear in the place of logarithm, decreases the heat of adsorption, ignoring extremely high and low concentrations. B is a constant relating to the heat of adsorption, with the expression $B = {}^{RT}/_{b}$, A is Temkin constants (L/g). A and B can be evaluated from intercept (BlnA) and slope (B) respectively.

Table 2
kinetic models used in this study.

Kinetics	Linear equation	Plot	Important parameter	Reference
Pseudo first order	$\ln(q_t - q_e) = lnq_e - k_1 t$	$\ln(q_t - q_e)$ *vs* t	k_i, q_{cal}	[39]
Pseudo second order	$\frac{t}{q_t} = \frac{1}{k_2 q_e^2} + \frac{1}{q_e} t$	$\frac{t}{q_t}$ *vs* t	k_2, q_e	[40]
Intraparticle diffusion	$q_t = k_{id} t_e^{\frac{1}{2}} + C$	q_t *vs* $\sqrt{t}$	k_{id}	[41]
Elovich	$q = \frac{1}{\beta}\ln(\alpha\beta) + \frac{1}{\beta} lnt$	q *vs* t	α, β	[42]

q_e and q_t are the amount of adsorbate adsorbed per mass of adsorbent at equilibrium and at time t (min) respectively, K_1 is the rate constant of the pseudo-first-order equation (min^{-1}), K_2 (g/mg min) is the equation rate constant for the pseudo-second-order model, k_{id} is the rate constant of the intraparticle diffusion with dimension mg/g min$^{1/2}$, C is the constant (the thickness of the boundary layer surrounding the adsorbent) (mg/g), α is the initial rate of adsorption and β is the desorption constant related to the extent of surface coverage and activation energy for chemisorption.

Adsorption operational parameters validation

The statistical analysis tool employed in this study is the R software. The relationship existing between equilibrium time, concentration and, quantity adsorbed was established using the Pearson correlation coefficient. The regression model was adopted to model the relationship between quantity adsorbed and the following predictors: concentration and equilibrium time. A preliminary evaluation was carried out by regressing quantity adsorbed on its predictors using the method of Ordinary Least Squares (OLS).

Results and discussion

Surface area and surface charge analysis

The adsorbent pore structure and surface chemistry were pivotal to the effectiveness of the adsorption process. Table 3 shows the Brunauer-Emmet-Teller analysis of CQES and RQES. Calcination greatly enhanced the surface area of the quail egg shells with about 50% increase. The surface area of RQES recorded to be 680.80 m^2/g increased to 927.30 m^2/g after calcination. Calcination process has been previously reported to increase surface area and porosity [43]. The pore sizes of 28.40 nm and 32.95 nm were obtained for RQES and CQES respectively (Table 3) falls within the mesoporous range, this indicates that both adsorbent will effectively provide percolation space for large molecules such as acetaminophens [44].

Table 3
Porosity and surface area analysis.

Adsorbent	Pore size (nm)	Surface area (m^2/g)
RQES	28.40	680.80
CQES	32.95	927.30

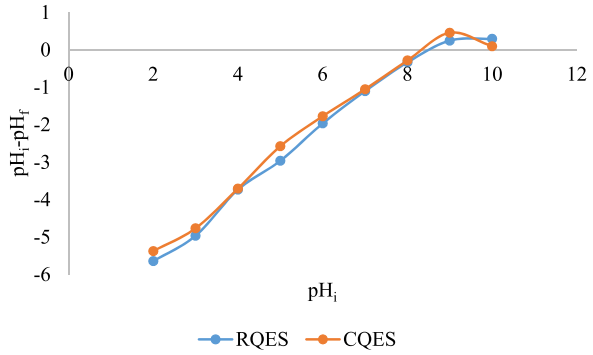

Fig. 2. pHpzc curve for (a) RQES and (b) CQES.

The pH point of zero charge (pH_{pzc}) analysis investigates the surface charge of RQES and CQES. The pHpzc of both adsorbents existed in the basic region viz 8.5 and 8.3 for RQES and CQES respectively as shown in Fig. 2(a) and (b). The negative surface of both adsorbents would provide a suitable surface for the uptake of cationic specie. Acetaminophen is a weak acid existing with pKa of 9.38 hence can exist in both non-ionized and ionized forms. Its acidic and basic distribution is greatly dependent on pH [45].

Fourier transformed infrared spectroscopy (FTIR)

Functional groups contribute greatly to the uptake of pollutants from wastewater. Band shift cum changes in band intensity justifies functional groups participation in adsorption. FTIR analysis of the RQES and CQES are presented as Figs. 3a-d; these shows the spectroscopic features of the adsorbents with major peaks influencing the process of adsorption. It also suggests the possible interaction mechanism of PCM with RQES and CQES adsorbents surfaces. Notable absorption bands observed in RQES include –OH stretching vibration at 3446 cm^{-1} (Figs. 3a) which may arise from adventitious water vibrations. A sharp absorption band was also observed at 3642 cm^{-1} in RQES, depicting N–H stretching vibrations of an amino group. Protein is a major component of the residual organic materials in eggshells [46]. In addition, a wide absorption band observed at about 1455 cm^{-1} may be linked to the carbonate minerals in the matrix of eggshells or the NH_2 scissoring of the residual proteins [47]. Other bands confirming calcium carbonate presence in RQES were observed at 874 cm^{-1} indicating out-plane and 708 cm^{-1}; indicating in-plane deformation modes of $CaCO_3$. The corroborative amine or amide absorption bands was observed at 1796 cm^{-1} in RQES. Calcined quail eggshells also showed characteristics absorption bands of amine/amide and calcium carbonate/calcium oxides and, Si-O at 3426, 1684, 1199 and 1050 cm^{-1} (Figs. 3b). Reduction in absorption band intensities were observed after PCM uptake for both RQES and CQES (Figs. 3a and b). A vivid absorption band appeared at 1012 cm^{-1} in RQES after PCM uptake which may be attributed to C–O stretching and C–N stretching vibrations. Previous reports suggests that such new appearance of absorption band after PCM uptake indicates the stability of PCM on the adsorbent surface [1].

Scanning electron microscopy (SEM)

Surface morphological appearance of RQES and CQES before and after PCM uptake are shown in Figs. 4a & b and Figs. 5a & b respectively. RQES had pores of various sizes before PCM uptake (Fig. 4a). Similar pores distributions were observed on CQES surface before PCM adsorption (Fig. 5a). The rough surfaces and heterogeneous pores would provide spaces for trapping the PCM molecules [17,20,48]. RQES and CQES surfaces had very scanty pores after PCM uptake.

Energy dispersive X-ray spectroscopic study (EDX)

EDX analysis which gave the elemental composition of both RQES and CQES. The EDX spectral of RQES and CQES are presented in Figs. 6a and b respectively. The high percentage of Ca^{2+} (55.1% and 48.8% for RQES and CQES respectively) is typical for eggshell. Calcination of RQES resulted into a slight decrease in percentage oxygen while the carbon content was enriched by about 30%.

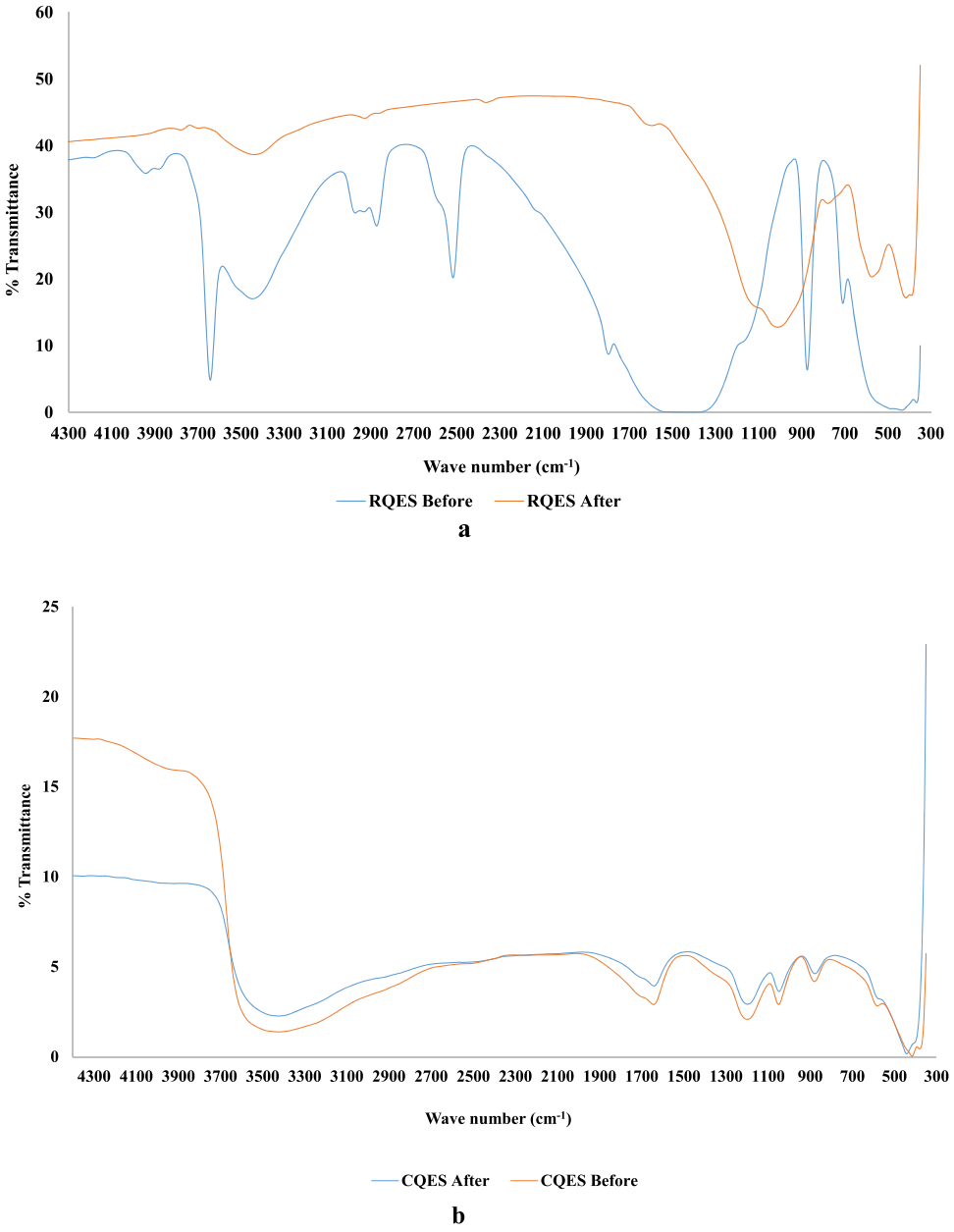

Fig. 3. a. FTIR spectra of RQES before and after the uptake of PCM and b. FTIR spectra of CQES before and after the uptake of PCM.

Various operational parameter effects on PCM uptake onto RQES and CQES

pH effect

The uptake of PCM onto RQES and CQES at varying solution pH is presented in Fig. 7. pH effects on PCM adsorption has not been well explored therefore some researchers did focus on selected pH studies [30]. However, pH is of great importance in adsorption studies. PCM can exist in both ionized and a non-ionized forms, and the acidic or basic distribution is strictly pH dependent [48,49]. The optimum percentage adsorption of PCM onto RQES and CQES were 86.29 and 83.83 at pH 7 and 6 respectively. PCM uptake decreased at higher pH, this can be attributed to the deprotonation of PCM. Percentage adsorption was observed to rise gradually until maximum adsorption was obtained at pH of 6 for CQES and pH of 7 for RQES. The pHpzc of RQES and CQES were obtained to be 8.5 and 8.3 respectively hence adsorbent surface is expected to be positively charged at lower pH and negatively charged at pH greater than pHpzc. Also at the lower pH, PCM would exist in its protonated form up to pH of 7, hence adsorption efficiency rises with pH up to pH of 7 [50]. The phenol group is subsequently deprotonated and above PCM's pKa (9.38), PCM molecules will exists in its deprotonated form hence attraction

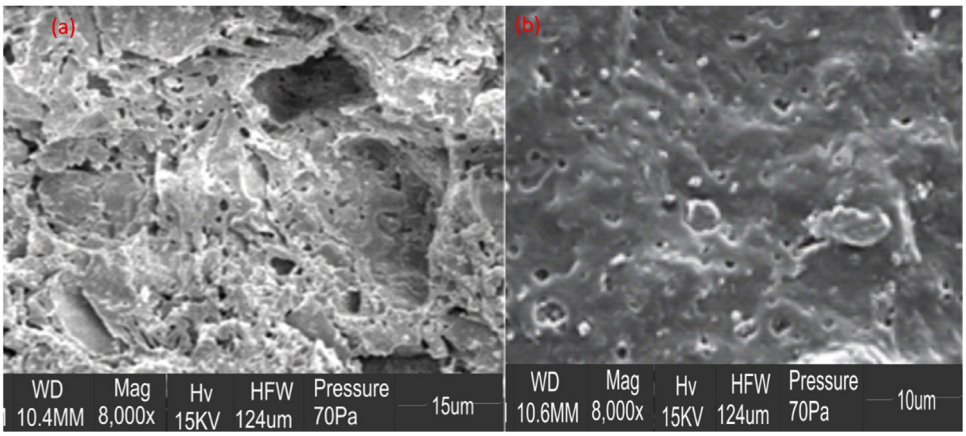

Fig. 4. RQES before adsorption (a) and RQES after adsorption (b).

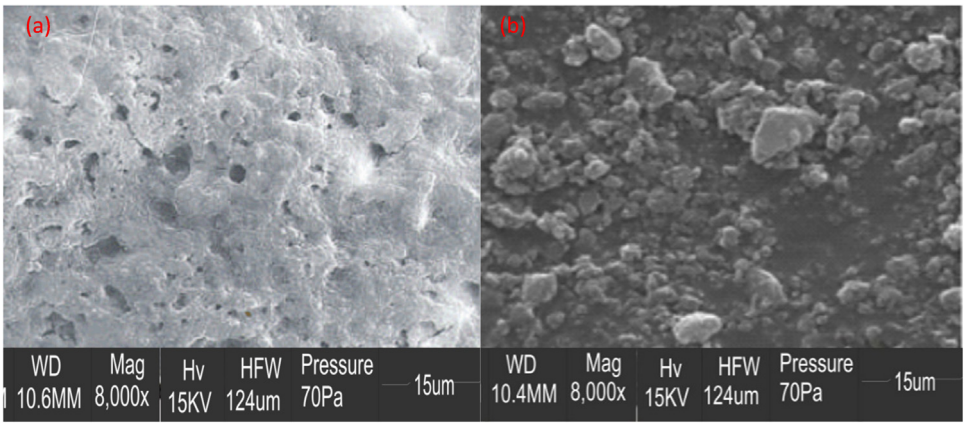

Fig. 5. CQES before adsorption (a) and CQES after adsorption (b).

towards adsorbent's surface drops drastically due to repulsion of like charges. The existence of PCM in its non-ionized form facilitated higher adsorption at low pH while electrostatic repulsion resulted in decrease adsorption at more basic media [31,52,53].

Initial concentration and contact time effect

Increased driving force provided by increased concentration of PCM in solution resulted to higher adsorption at higher initial PCM concentrations (Figs. 8a and b). A huge percentage of the total PCM adsorption within the 120 min kinetics occurred within the first 20 min. The rapid initial adsorption of PCM unto RQES and CQES subsequently slowly goes to equilibrium. The initial rapid adsorption of PCM unto the adsorbent surface may have occurred due to numerous numbers of active sites on the fresh adsorbents as well as the presence of many molecules of PCM at the initial time. Rapid adsorption kinetics within the first 20 min has previously been reported [45].

Isothermal studies of PCM adsorption unto RQES and CQES

Adsorption data for the uptake of PCM unto RQES fitted well to Freundlich adsorption isotherm suggesting that uptake of PCM was unto multi-surface. The multi-surface adsorption observed may have occurred in stages; first to the available surface adsorption sites followed by adsorbate-adsorbate interactions. The adsorbate-adsorbate interactions were accounted for by the high R^2 value obtained for Temkin adsorption isotherm. The Dubinin-Radushkevich model provided the best fit for the uptake of PCM onto CQES; although in Langmuir/Freundlich comparison, multilayer adsorption also occurred in the CQES-PCM system. The favorability of PCM uptake onto RQES and CQES was established by the values of dimensionless R_L (Table 4). The D-R values for energy of adsorption obtained for the RQES-PCM and CQES-PCM interactions were 23.57 and 8.54 $KJmol^{-1}$ respectively suggesting that chemisorption process occurred in both systems. The qe obtained for both RQES and CQES were 10.64 and 9.89 mg/g respectively. Also the maximum monolayer adsorption capacities were obtained to

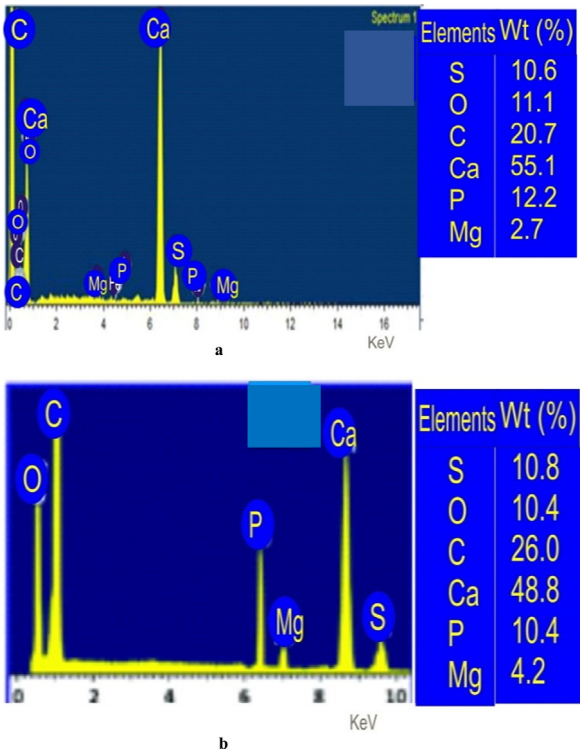

Fig. 6. a. EDX spectrum of RQES b. EDX spectrum of CQES.

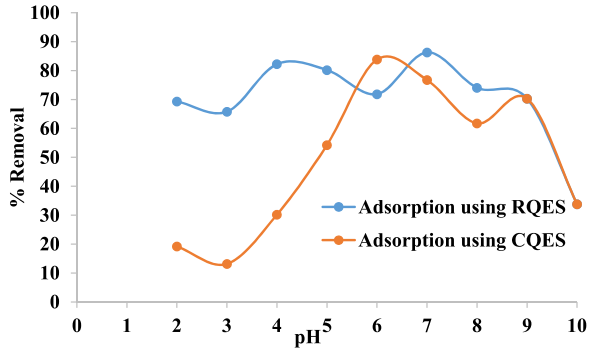

Fig. 7. pH effects (operational conditions: adsorbent dosage (1 g/L), temperature (26 ± 2 °C), contact time (120 min), initial adsorbate concentration (6 mg/L) and agitation speed (130 rpm).

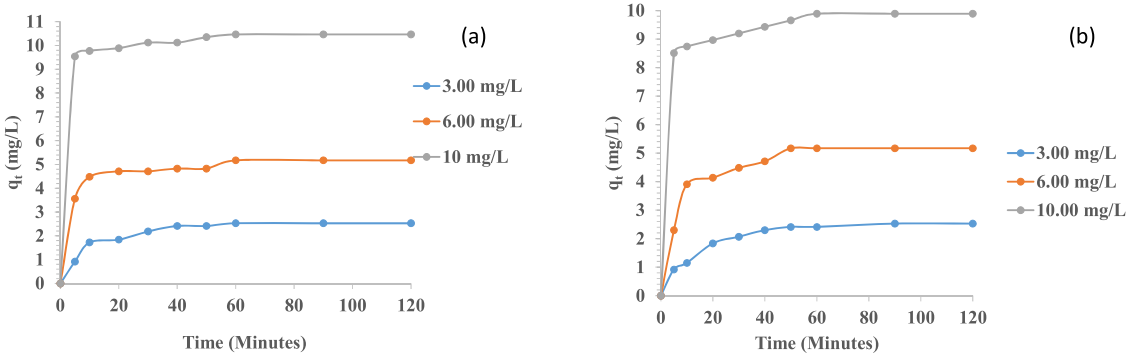

Fig. 8. Effects of Concentration and contact time on paracetamol adsorption unto (a) RQES and (b) CQES respectively (operational conditions: pH (7 & 6 for a & b respectively), adsorbent dosage (1 g/L), temperature (26 ± 2 °C), and agitation speed (130 rpm).

Table 4
Isotherm parameters of PCM adsorption unto RQES and CQES.

Isotherms	constants	RQES	CQES
Langmuir	q_{max} (mg/g)	10.00	15.15
	R^2	0.9362	0.8919
	R_L	0.05169	0.06371
	K_L (L.mg^{-1})	1.7391	1.3983
Freundlich	K_F	0.1686	0.0865
	R^2	0.9999	0.9793
	n	0.7392	1.0064
Temkin	A (L/g)	8.1721	0.8183
	R^2	0.9582	0.9979
	b (J/mol)	334.33	459.53
	B	7.535	5.482
D-R	q_o (mg/g)	20.43	15.08
	R^2	0.9861	1.0000
	E (KJmol^{-1})	23.57	8.4515
	β(mol^2.KJ^{-2})	0.0009	0.007

Table 5
Comparing previously reported maximum adsorption capacities of various adsorbents used in the removal of PCM.

Adsorbents	q_{max} (mg/g)	References
Rice husks	7.65	[50]
Oil palm fiber	7.30	[54]
Iron nanoparticles	11.627	[55]
Hemp activated carbon	16.18	[51]
Composite geomaterial	14.67	[56]
Sugar cane bagasse	0.32	[57]
Corn cob	0.47	[57]
Horse chest nut shell	1.091	[58]
Raw quail egg shells	10.00	This study
Calcined quail egg shells	15.15	This study

be 10.00 mg/g and 15.15 mg/g for RQES-PCM and CQES-PCM respectively. These have been compared with other previous works reported (Table 5). RQES and CQES was found efficient.

Whereas, for CQES, the Dubinin-Radushkevich model provided the best fit

Kinetic studies

The kinetics of PCM uptake unto RQES and CQES was observed to be first rapid and subsequently went to equilibrium. The pseudo-second-order kinetics model best explain the adsorption kinetic data. The quantity at equilibrium calculated ($q_{e\ calculated}$) for the pseudo-second-order closely agree with experimentally obtained quantity at equilibrium ($q_{e\ experimental}$) (Table 6). In addition to the immediate aforementioned, the high correlation coefficient of the pseudo-second-order kinetics analysis further subtantiate that the RQES-PCM and CQES-PCM are controlled by the pseudo-second-order kinetics. This suggested that chemisorption governed the uptake of PCM unto RQES and CQES [59]. The correlation coefficients for the Elovich kinetics models are well over 0.8 across concentrations considered for both RQES-PCM and CQES-PCM systems hence further support to the pseudo-second-order kinetics. This further confirmed that RQES-PCM and CQES-PCM ran on chemisorption and the chemisorption rate (α_{El}) increased with concentration. Although the intra-particle diffusion was not the rate limiting step as the q_t versus $t^{½}$ did not pass through the origin (Figure not shown). The boundary layer thickness was observed to increase with concentration.

Adsorbent loading effect

Percentage PCM removal was found to be highest at a dosage of 1 g/L of RQES and CQES (Fig. 9). Optimum percentage PCM removal were 90.75% and 73.63% for RQES and CQES respectively. Overlap of adsorbents may have resulted into blockage of many adsorption sites at high adsorbent dosage hence, the low PCM removal at higher adsorbent dosage.

Temperature effect

PCM percentage uptake unto CQES increased from 57.60 to 69.12% as temperature of the system increased from 30 to 50 °C (Fig. 10). This suggests that there is rapid mobility of PCM molecules to interact with the active sites of CQES adsorbents as temperature increased. Decrease in viscosity at high system temperature, aided increased mobility of PCM molecule to break through the internal and external boundaries on the adsorbent surfaces. Hence, CQES trapped more PCM molecules

Table 6
Kinetic studies of PCM adsorption onto RQES and CQES.

Constants	Initial concentration (mg/L)					
	RQES			CQES		
	3.0000	6.0000	10.0000	3.0000	6.0000	10.0000
$q_{e\ exp.}$ (mg/g)	2.5281	5.1721	10.464	2.5281	5.1721	9.8893
Pseudo first order						
$q_{e\ cal.}$ (mg/L)	1.8953	1.1538	1.1636	2.1016	2.7137	1.7668
$K_1 \times 10^{-2}$ (min^{-1})	6.0300	2.8600	4.0100	5.2800	4.5900	3.7100
R^2	0.9436	0.7317	0.8987	0.9766	0.9051	0.9561
Pseudo second order						
$q_{e\ cal.}$ (mg/g)	2.6645	5.2466	10.5263	2.7108	5.3793	9.9900
$K_2 \times 10^{-2}$ ($gmg^{-1}min^{-1}$)	6.8840	8.8490	12.1470	4.7270	4.5500	7.0500
R^2	0.9950	0.9989	0.9998	0.9920	0.9970	0.9995
Elovich						
α_{El} (mg/g.min)	1.0781	482.731	61.33×10^{10}	0.6114	4.7845	2.229×10^{6}
β_{El}(g/mg)	2.004	2.2051	3.1348	1.7593	1.1616	2.0092
R^2	0.8972	0.8602	0.9487	0.9419	0.8766	0.9469
Intra particle diffusion						
C (mgg^{-1})	1.0848	3.7875	9.4286	0.8118	2.69	8.2419
$K_{diff.}$ ($mgg^{-1}min^{-1/2}$)	0.1636	0.1502	0.1112	0.1906	0.2813	0.1756
R^2	0.7371	0.7219	0.8815	0.8098	0.7160	0.9017

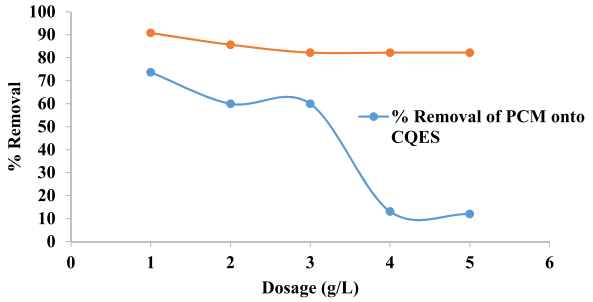

Fig. 9. Effects of adsorbent loading on PCM adsorption unto RQES and CQES (operational conditions: pH (7 & 6 for a & b respectively), temperature (26 ± 2 °C), contact time (120 min), agitation speed (130 rpm) and initial adsorbate concentration (6 mg/L).

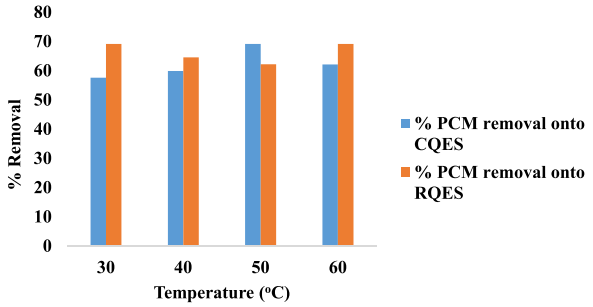

Fig. 10. Effects of temperature on PCM adsorption unto RQES and CQES (operational conditions: adsorbent load (1 g/L), pH (7 & 6 for a & b respectively), contact time (120 min), speed (130 rpm) and initial adsorbate concentration (6 mg/L).

at higher temperature. Percentage PCM uptake unto CQES however dropped from 69.12% to 62.12% as temperature changed from 50 °C to 60 °C; previous report states that adsorbate which are weakly bonded to adsorbent surface may lose their attachment at high temperature resulting in sudden decrease adsorption quantity [60]. In the RQES-PCM system, the uptake of PCM decreased from 69.12 to 62.21% with increase in system temperature from 30 to 50 °C. The adsorption of PCM unto RQES subsequently increased to 69.12% as the temperature increased to 60 °C. Activation of some adsorption site is said to occur at high temperature hence increase adsorption capacity [61]. Depending on system activity viz-a-viz temperature suggests either an exothermic or endothermic process [20,62].

Table 7
Thermodynamics studies of PCM adsorption onto RQES and CQES.

Adsorbents	ΔH^o (KJmol^{-1})	ΔS^o (Jmol^{-1}K^{-1})	ΔG^o (KJmol^{-1})			
			313	323	333	343
RQES	−193.3	0.027	−0.202	−0.1988	−0.2072	−0.402
CQES	279.08	11.45	−0.0765	−0.1336	−0.335	−0.404

Table 8
Correlation analysis output.

	CONC	EQUI	QUAD
CON	1	.450	.994
EQUI	.450	1	.400
QUA	.994	−0.400	1

Table 9
Diagnostic check using OLSE.

Variables	Coef	Eigenvalue	Condition Index
Intercept.	−2.176	2.834	1.000
Concentration.	1.131	.154	4.288
Equilibrium time.	0.015	.012	15.639
R^2	0.991	F-test	172.129 (0.001)

Table 10
Validation Output.

Coef.	OLSE	Ridge
Intercept.	0.1220	0.2671
Concentration.	0.9864	0.5979
Equilibrium time.	0.2500	0.3243
TMSE.	0.3349	0.1166

Thermodynamic studies

The positive values of $\Delta \mathbf{S^o}$ indicate an increase in the randomness of the adsorption process as it approached equilibrium. Increased randomness at the solid-liquid interface may be attributed to the possibility of the displaced water possessing a higher translational entropy than that lost during the uptake of PCM. The negative value of ΔH° for RQES indicates an exothermic process while that of CQES is endothermic. The feasibility of the adsorption systems were established by the negative values of calculated ΔG^o (Table 7). Process feasibility increased with increase in temperature [62–64].

Statistical validation

The result in Table 8 revealed a strong positive relationship between quantity adsorbed and concentration. This further validates the possibility of a higher driving force at higher concentration with consequential increased quantity adsorbed. There is a low positive correlation between the following pairs: concentration and equilibrium time, equilibrium time and, quantity adsorbed. This established the fact that at equilibrium time only slight increase in quantity adsorbed may have been recorded. The estimate of Ordinary Least Square (OLS) and its diagnostic result are available in Table 9. The F-test shows that the fitted model fits the data well. Concentration and equilibrium time explains approximately 99% of the variation in quantity adsorbed (R^2=0.991). However, following [65], when R^2 exceeds 0.8, there is tendency that the model suffers from the problem of multicollinearity. Multicollinearity is a threat to the performance of the method of ordinary least squares [66–69]. The use of condition index is a more formal way to assess if a model suffers multicollinearity [70]. When the condition index (CI) is between 10 and 30, it is evident that there is multicollinearity. The CI in Table 9 is 15.639, which shows there is multicollinearity. The ridge estimator was adopted for effective modeling [71,72]. See [72,73] for the cross-validation procedure. The model performance is judged using the test mean squared error (TMSE). The regression coefficients, estimated test mean squared error are reported in Table 10. The test mean squared error supported the use of the ridge estimator as alternative to the OLS because it gives a smaller TMSE (0.1166). There is about 65% change in the value of the OLS TMSE to the ridge TMSE. We observed that quantity adsorbed rises by about 60% as concentration increased and by 32% as time increased. This suggests efficient performance of the prepared adsorbents in the phase of highly polluted aqueous effluent. In addition, the high percentage increase in quantity adsorbed with time greatly justify the economy of operational processes.

Table 11a
Regression Output of Quantity adsorbed on Temperature RQES.

Model		Unstandardized Coefficients		t	Sig.
		B	Std. Error		
1	(Constant)	67.282	8.739	7.699	0.016
	Temperature	−0.023	0.188	−0.123	0.914

Table 11b
Regression Output of Quantity adsorbed on CQES.

Model		Unstandardized Coefficients		t	Sig.
		B	Std. Error		
1	(Constant)	51.941	10.198	5.093	0.036
	Temperature	0.228	0.220	1.035	0.409

Table 12
t-test for Equality of Means.

t	df	Sig. (2-tailed)	Mean Difference	Std. Error Difference
−1.339	6	0.229	−4.055	3.02881
−1.339	5.346	0.235	−4.055	3.02881

Table 13
Regression Output of Quad. on time.

Quad Type	Concentration	Model	Unstandardized Coefficients		t	sig
			B	Std. Error		
Calcined	3ppm	Intercept	1.090	0.276	3.946	0.004
		Time	0.017	0.005	3.477	0.008
	6ppm	Intercept	2.764	0.622	4.447	0.002
		Time	0.030	0.011	2.680	0.028
	10ppm	Intercept	6.731	1.318	5.107	0.001
		Time	0.040	0.023	1.693	0.029
Raw	3ppm	Intercept	1.239	0.298	4.159	0.003
		Time	0.016	0.005	2.967	0.018
	6ppm	Intercept	3.271	0.657	4.976	0.001
		Time	0.023	0.012	1.999	0.081
	10ppm	Intercept	7.493	1.463	5.121	0.001
		Time	0.038	0.026	1.470	0.030

The regression analysis output in Table 11a and 11b shows that temperature effect on the quantity of PCM adsorbed onto RQES and CQES vary. For instance, as the temperature increase in Table 9, quantity adsorbed onto CQES increases by 22.8 percent. This shows a huge compensation for economy viz-a-viz energy consumption. The temperature effect however showed a reverse trend in the RQES-PCM system. With increase in temperature, quantity adsorbed onto RQES decreased by about 2 percent (Table 11a). The RQES-PCM is therefore better to run at ordinary room temperature. We examined if there is significant difference between the quantity of PCM adsorbed onto CQES and RQES using the *t*-test. The result is provided in Table 12. The result shows there is no significant difference between the mean of PCM quantity adsorbed onto CQES and RQES. Table 13 presents the effect of time on the quantity of PCM adsorbed at varying concentrations. The highest time impact was observed at 10 ppm and lowest at 3 ppm for CQES. The results follow a similar trend for RQES-PCM system.

Conclusion

Adsorbents prepared from quail eggshells were investigated for the uptake of PCM. The porosities of the prepared adsorbents indicated suitability for large molecule uptake and this was validated. Uptake of PCM was pH-dependent and optimum pH were 7 and 6 for RQES and CQES respectively. PCM removal was more favorable at high temperature for the CQES-PCM system while the RQES-PCM system would work better at ordinary room temperature. Adsorption of PCM to the adsorbent surfaces occurred via the chemisorption process. The negative values of ΔG^o established the feasibility of the adsorption process and feasibility was observed to increase with temperature. Strong correlation exists between quantity adsorbed and concentration, therefore justifying the strong driving force that is usually experienced at higher concentration. About 32% increase in quantity adsorbed with changes in time accounted for great economic advantage viz-a-viz process time. Percentage PCM removal increase to the tone of 22.8% per unit increase in temperature showed a huge compensation for energy cost hence a justification for economical process. Therefore, in addition to the low cost of RQES and CQES; their PCM re-

moval efficiency cum percentage increase viz-a-viz time and temperature changes greatly justified the economic advantage of these adsorption processes. Economy advantage of the adsorption process would be of great interest to the low- and middle-income nations. The utilization of agricultural waste in adsorption process is green and would provide access to safety and sustainability. Hence, the findings of this research serve as an important tool in achieving a target in the quest for a "Prosperous Africa" an Africa's Union's Agenda 2063; as well the drive for Clean Water and Sanitation Sustainable Development Goal.

Declaration of Competing Interest

The authors declare that they have no known competing financial interests or personal relationships that could have appeared to influence the work reported in this paper.

References

[1] L. Spessato, C. Bedina, K. Andre, L.C. Souzaa, P.A.F. Vitor, A.D. Crespoa, L.C.H. Marcela, C.S. Pontesa, M Almeida R, C. Vitor, KOH-super activated carbon from biomass waste: insights into the paracetamol adsorption mechanism and thermal regeneration cycles, J. Hazard. Mater. 371 (2018) 499–505 December2019, doi:10.1016/j.jhazmat.2019.02.102.

[2] I.C. Afolabi, S.I. Popoola, O.S. Bello, Modeling pseudo-second-order kinetics of orange peel-paracetamol adsorption process using artificial neural network, Chemom. Intell. Lab. Syst. 203 (2020) 104053 January, doi:10.1016/j.chemolab.2020.104053.

[3] L. Sellaoui, E.C. Lima, G.L. Dotto, A. Ben Lamine, Adsorption of amoxicillin and paracetamol on modified activated carbons: equilibrium and positional entropy studies, J. Mol. Liq. 234 (2017) 375–381, doi:10.1016/j.molliq.2017.03.111.

[4] D.R. Lima, A. Hosseini-Bandegharaei, P.S. Thue, E.C. Lima, Y.R.T. de Albuquerque, G.S. dos Reis, G.S. Umpierres, C.S. Dias, S.L.P. Tran, H. Nguyen, Efficient acetaminophen removal from water and hospital effluents treatment by activated carbons derived from Brazil nutshells, Colloids Surf. A Physicochem. Eng. Asp. 583 (2019) 123966 September, doi:10.1016/j.colsurfa.2019.123966.

[5] J. Żur, D. Wojcieszyńska, K. Hupert-Kocurek, A. Marchlewicz, U. Guzik, Paracetamol – toxicity and microbial utilization. Pseudomonas moorei KB4 as a case study for exploring degradation pathway, Chemosphere 206 (2018) 192–202, doi:10.1016/j.chemosphere.2018.04.179.

[6] A. Bertolini, A. Ferrari, A. Ottani, S. Guerzoni, R. Tacchi, S. Leone, Paracetamol: new vistas of an old drug, CNS Drug Rev 12 (3–4) (2006) 250–275, doi:10.1111/j.1527-3458.2006.00250.x.

[7] W. Koagouw, Z. Arifin, G.W.J. Olivier, C. Ciocan, High concentrations of paracetamol in effluent dominated waters of Jakarta Bay, Indonesia, Mar. Pollut. Bull. 169 (2021) 112558 June, doi:10.1016/j.marpolbul.2021.112558.

[8] N. Pi, J.Z. Ng, B.C. Kelly, Bioaccumulation of pharmaceutically active compounds and endocrine disrupting chemicals in aquatic macrophytes: results of hydroponic experiments with Echinodorus horemanii and Eichhornia crassipes, Sci. Total Environ. 601–602 (1) (2017) 812–820, doi:10.1016/j.scitotenv.2017.05.137.

[9] N. Boudrahem, S. Delpeux-Ouldriane, L. Khenniche, F. Boudrahem, F. Aissani-Benissad, M. Gineys, Single and mixture adsorption of clofibric acid, tetracycline and paracetamol onto Activated carbon developed from cotton cloth residue, Process Saf. Environ. Prot. 111 (2017) 544–559, doi:10.1016/j.psep.2017.08.025.

[10] A.S. Ramos, A.T. Correia, S.C. Antunes, F. Gonçalves, B. Nunes, Effect of acetaminophen exposure in oncorhynchus mykiss gills and liver: detoxification mechanisms, oxidative defence system and peroxidative damage, Environ. Toxicol. Pharmacol. 37 (3) (2014) 1221–1228, doi:10.1016/j.etap.2014.04.005.

[11] R. Anjali, S. Shanthakumar, Insights on the current status of occurrence and removal of antibiotics in wastewater by advanced oxidation processes, J. Environ. Manage. 246 (2019) 51–62 January, doi:10.1016/j.jenvman.2019.05.090.

[12] Y. Gu, J. Huang, G. Zeng, L. Shi, Y. Shi, K. Yi, Fate of pharmaceuticals during membrane bioreactor treatment: status and perspectives, Bioresour. Technol. 268 (2018) 733–748 June, doi:10.1016/j.biortech.2018.08.029.

[13] P. Song, Z. Yang, G. Zeng, X. Yang, H. Xu, L. Wang, R. Xu, W. Xiong, K. Ahmad, Electrocoagulation treatment of arsenic in wastewaters: a comprehensive review, Chem. Eng. J. 317 (2017) 707–725, doi:10.1016/j.cej.2017.02.086.

[14] O.S. Bello, T.C. Alagbada, O.C. Alao, A.M. Olatunde, Sequestering a non-steroidal anti-inflammatory drug using modified orange peels, Appl. Water Sci. 10 (7) (2020), doi:10.1007/s13201-020-01254-8.

[15] O.S. Bello, M.A. Moshood, B.A. Ewetumo, I.C. Afolabi, Ibuprofen removal using coconut husk activated Biomass, Chem. Data Collect. 29 (2020), doi:10.1016/j.cdc.2020.100533.

[16] A.O. Dada, F.A. Adekola, E.O. Odebunmi, Kinetics, mechanism, isotherm and thermodynamic studies of liquid phase adsorption of Pb 2+ onto wood activated carbon supported zerovalent iron (WAC-ZVI) nanocomposite, Cogent Chem 3 (1) (2017) 1351653, doi:10.1080/23312009.2017.1351653.

[17] A.A. Inyinbor, F.A. Adekola, G.A. Olatunji, Microwave-assisted urea modified crop residue in Cu2+ scavenging, Heliyon 6 (4) (2020) e03759, doi:10.1016/j.heliyon.2020.e03759.

[18] A.A. Inyinbor, F.A. Adekola, A.O. Dada, A.P. Oluyori, G.A. Olatunji, F.O. Fanawopo, T.O. Oreofe, Novel acid treated biomass: applications in Cu[Formula presented] scavenging, Rhodamine B/Cu[Formula presented] binary solution and real textile effluent treatment, Environ. Technol. Innov. 13 (2019) 37–47, doi:10.1016/j.eti.2018.10.006.

[19] A.A. Inyinbor, F.A. Adekola, G.A. Olatunji, Low cost adsorbent prepared from Vigna subterranean waste: physicochemical, morphological and surface chemistry data set, Chem. Data Collect. 24 (2019) 100294, doi:10.1016/j.cdc.2019.100294.

[20] O.S. Bello, E.O. Alabi, K.A. Adegoke, S.A. Adegboyega, A.A. Inyinbor, A.O. Dada, Rhodamine B dye sequestration using Gmelina aborea leaf powder, Heliyon 6 (1) (2020) e02872, doi:10.1016/j.heliyon.2019.e02872.

[21] S. Wong, Y. Ngadi, N. Mat, R. Hassan, O. Inuwa, I.M. Mohamed, N.B. Low, J. Horet, Removal of acetaminophen by activated carbon synthesized from spent tea leaves: equilibrium, kinetics and thermodynamics studies, Powder Technol 338 (2018) 878–886, doi:10.1016/j.powtec.2018.07.075.

[22] K.S. Obayomi, J.O. Bello, M.D. Yahya, E. Chukwunedum, J.B. Adeoye, Statistical analyses on effective removal of cadmium and hexavalent chromium ions by multiwall carbon nanotubes (MWCNTs, Heliyon 6 (6) (2020) e04174, doi:10.1016/j.heliyon.2020.e04174.

[23] M.A. Abdel-Khalek, M.K. Abdel Rahman, A.A. Francis, Exploring the adsorption behavior of cationic and anionic dyes on industrial waste shells of egg, J. Environ. Chem. Eng. 5 (1) (2017) 319–327, doi:10.1016/j.jece.2016.11.043.

[24] O.S. Bello, O.C. Alao, T.C. Alagbada, O.S. Agboola, O.T. Omotoba, O.R. Abikoye, A renewable, sustainable and low-cost adsorbent for ibuprofen removal, Water Science and Technology 83 (1) (2021) 111–122, doi:10.2166/wst.2020.551.

[25] A. Bambaeero, R. Bazargan-Lari, Simultaneous removal of copper and zinc ions by low cost natural snail shell/hydroxyapatite/chitosan composite, Chinese J. Chem. Eng. 33 (2021) 221–230, doi:10.1016/j.cjche.2020.07.066.

[26] Y.G. Reddy, T.B. Narsaiah, B.V. Rao, Low cost adsorbents utilization for the treatment of pharmaceutical wastewater, Int. J. Civ. Eng. Res. 2 (3) (2017) 339–341.

[27] K. Li, Z. Rong, Y. Li, C. Li, Z. Zheng, Preparation of nitrogen-doped cotton stalk microporous activated carbon fiber electrodes with different surface area from hexamethylenetetramine-modified cotton stalk for electrochemical degradation of methylene blue, Results Phys 7 (2017) 656–664, doi:10.1016/j.rinp.2017.01.030.

[28] A.B. Leite, C. Saucier, E.C. Lima, C.S. dos Reis, G.S. Umpierres, C.S. Mello, B.L. Shirmardi, M. Dias, L.P. Silvio, C.H. Sampaio, C. H, Activated carbons from avocado seed: optimisation and application for removal of several emerging organic compounds, Environ. Sci. Pollut. Res. 25 (8) (2018) 7647–7661, doi:10.1007/s11356-017-1105-9.

[29] Y. Shi, G. Liu, M. Li, L. Wang, Egg shell waste as an activation agent for the manufacture of porous carbon, Chinese J. Chem. Eng. 28 (3) (2020) 896–900, doi:10.1016/j.cjche.2019.09.014.

[30] A. Muhammad-Lawal, K.B. Amolegbe, O.A. Abdulsalam, Economics of quail production in Ilorin, Kwara State, Nigeria, J. Agric. Ext. 21 (2) (2017) 44–53, doi:10.4314/jae.v21i2.4.

[31] S. Parvin, B.K. Biswas, M.A. Rahman, M.H. Rahman, M.S. Anik, M.R. Uddin, Study on adsorption of Congo red onto chemically modified egg shell membrane, Chemosphere 236 (2019), doi:10.1016/j.chemosphere.2019.07.057.

[32] A. Ahmad, D. Jini, M. Aravind, C. Parvathiraja, R. Ali, M.Z. Kiyani, A. Alothman, A novel study on synthesis of egg shell based activated carbon for degradation of methylene blue via photocatalysis, Arab. J. Chem. 13 (12) (2020) 8717–8722, doi:10.1016/j.arabjc.2020.10.002.

[33] E. Panagiotou, N. Kafa, L. Koutsokeras, P. Kouis, P. Nikolaou, G. Constantinides, I. Vyrides, Turning calcined waste egg shells and wastewater to Brushite: phosphorus adsorption from aqua media and anaerobic sludge leach water, J. Clean. Prod. 178 (2018) 419–428, doi:10.1016/j.jclepro.2018.01.014.

[34] mohit nigam S. Rajoriya, V.K. Saharan, A.S. Pundir, K. Roy, Adsorption of methyl red dye from aqueous solution onto eggshell waste material: kinetics, isotherms and thermodynamic studies, SSRN Electron. J. (2021), doi:10.2139/ssrn.3910226.

[35] I. Langmuir, The constitution and fundamental properties of solids and liquids, J. Franklin Inst. 183 (1) (1917) 102–105, doi:10.1016/S0016-0032(17)90938-X.

[36] H.M... Freundlich, Over theadsorption in solution, Z. Phys. Chem. 57 (1906) 385–470.

[37] M.M..R.L.V. Dubinin, Equation of the characteristic curve of activated charcoal proceedings of the academy of sciences, Dokl. Akad. Nauk SSSR, Phys. Chem. Sect. USSR 55 (1947) 331–333.

[38] V. Tempkin, M.I. Pyzhev, Kinetics of ammonia synthesis on promoted iron catalyst, Acta Phys. Chim. USSR 12 (1940) 327–356.

[39] S. Lagergren, On the theory of so-called adsorption of dissolved substances, K. Sven. Vetenskapsakademiens Handl. 24 (4) (1898) 1–39.

[40] G.M.Y.S. Ho, Pseudo - second order model for sorption processes", Process Biochemistry, Process Biochem 34 (1999) 34, pp. 451–465, 1999.

[41] G. McKay, M.S. Otterburn, A.G. Sweeney, The removal of colour from effluent using various adsorbents-III. Silica: rate processes, Water Res 14 (1) (1980) 15–20, doi:10.1016/0043-1354(80)90037-8.

[42] C. Aharoni, M. Ungarish, Kinetics of activated chemisorption: part 1.-The non-elovichian part of the isotherm, J. Chem. Soc. Faraday Trans. 1 Phys. Chem. Condens. Phases 72 (1976) 400–408, doi:10.1039/F19767200400.

[43] L.T. Popoola, A.S. Yusuff, A.A. Adeyi, O.O. Omotara, Adsorptive removal of heavy metals from oil well produced water using citrullus lanatus peel: characterization and optimization, South African J. Chem. Eng. 39 (2022) 19–27, doi:10.1016/j.sajce.2021.11.001.

[44] A.A. Inyinbor, F.A. Adekola, G.A. Olatunji, Liquid phase adsorptions of Rhodamine B dye onto raw and chitosan supported mesoporous adsorbents: isotherms and kinetics studies, Appl. Water Sci. 7 (5) (2017) 2297–2307, doi:10.1007/s13201-016-0405-4.

[45] A. Gómez-Avilés, M. Peñas-Garzón, C. Belver, J.J. Rodriguez, J. Bedia, Equilibrium, kinetics and breakthrough curves of acetaminophen adsorption onto activated carbons from microwave-assisted FeCl3-activation of lignin, Sep. Purif. Technol. 278 (2022), doi:10.1016/j.seppur.2021.119654.

[46] A. Laca, A. Laca, M. Díaz, Eggshell waste as catalyst: a review, J. Environ. Manage. 197 (2017) 351–359, doi:10.1016/j.jenvman.2017.03.088.

[47] J. Carvalho, J. Araujo, F. Castro, Alternative low-cost adsorbent for water and wastewater decontamination derived from eggshell waste: an overview, Waste Biomass Valorizat. 2 (2) (2011) 157–167, doi:10.1007/s12649-010-9058-y.

[48] M.A. Ahmad, N.S. Afandi, K.A. Adegoke, O.S. Bello, Optimization and batch studies on adsorption of malachite green dye using rambutan seed activated carbon, Desalin. Water Treat. 57 (45) (2016) 21487–21511, doi:10.1080/19443994.2015.1119744.

[49] V. Bernal, A. Erto, L. Giraldo, J.C. Moreno-Piraján, Effect of solution pH on the adsorption of paracetamol on chemically modified activated carbons, Molecules 22 (7) (2017), doi:10.3390/molecules22071032.

[50] A. Thakur, N. Sharma, A. Mann, Removal of ofloxacin hydrochloride and paracetamol from aqueous solutions: binary mixtures and competitive adsorption, Mater. Today Proc. 28 (2) (2020) 1514–1519, doi:10.1016/j.matpr.2020.04.833.

[51] M. Sajid, S. Bari, M. Saif Ur Rehman, M. Ashfaq, Y. Guoliang, G. Mustafa, Adsorption characteristics of paracetamol removal onto activated carbon prepared from Cannabis sativum Hemp, Alexandria Eng. J. 61 (9) (2022) 7203–7212, doi:10.1016/j.aej.2021.12.060.

[52] M.R. Elamin, B.Y. Abdulkhair, A.O. Elzupir, Insight to aspirin sorption behavior on carbon nanotubes from aqueous solution: thermodynamics, kinetics, influence of functionalization and solution parameters, Sci. Rep. 9 (1) (2019), doi:10.1038/s41598-019-49331-6.

[53] R. Natarajan, K. Benerjee, P.S. Kumar, T. Somanna, D. Tannani, V. Arvind, R.I. Raj, D.N. Vo, K. Saikia, V.K. Vaidyanathan, Performance study on adsorptive removal of acetaminophen from wastewater using silica microspheres: kinetic and isotherm studies, Chemosphere 272 (2021), doi:10.1016/j.chemosphere.2021.129896.

[54] C.M. Grisales-Cifuentes, E.A. Serna Galvis, J. Porras, E. Flórez, R.A. Torres-Palma, N. Acelas, Kinetics, isotherms, effect of structure, and computational analysis during the removal of three representative pharmaceuticals from water by adsorption using a biochar obtained from oil palm fiber, Bioresour. Technol. 326 (2021), doi:10.1016/j.biortech.2021.124753.

[55] C.S. Praveen Kumar, V.P. Sylas, C. Neethu, V. Ambily, C.T. Sunila, N.P. Sreekanth, M.P. Rayaroth, Acetaminophen removal using green synthesized iron nanoparticles with a fresh water microalga, Planktochlorella nurekis, Nano-Struct. Nano-Obj. 26 (2021), doi:10.1016/j.nanoso.2021.100700.

[56] S.A. Hamoudi, M. Brahimi, M. Boucha, B. Hamdi, J. Arrar, Removal of paracetamol from aqueous solution by containment composites, Open Chem 19 (1) (2021) 49–59, doi:10.1515/chem-2020-0188.

[57] D.M. Juela, Comparison of the adsorption capacity of acetaminophen on sugarcane bagasse and corn cob by dynamic simulation, Sustain. Environ. Res. 30 (1) (2020), doi:10.1186/s42834-020-00063-7.

[58] A. Parus, M. Gaj, B. Karbowska, J. Zembrzuska, Investigation of acetaminophen adsorption with a biosorbent as a purification method of aqueous solution, Chem. Ecol. 36 (7) (2020) 705–725, doi:10.1080/02757540.2020.1757081.

[59] H.K. Agbovi, L.D. Wilson, Adsorption processes in biopolymer systems: fundamentals to practical applications, Nat. Polym. Green Adsorbents Water Treat. (2021) 1–51, doi:10.1016/b978-0-12-820541-9.00011-9.

[60] A.A. Inyinbor, F.A. Adekola, G.A. Olatunji, Adsorption of rhodamine b dye from aqueous solution on Irvingia gabonensis biomass: kinetics and thermodynamics studies, South African J. Chem. 68 (1) (2015) 115–125, doi:10.17159/0379-4350/2015/v68a17.

[61] A.A. Inyinbor, F.A. Adekola, G.A. Olatunji, Copper scavenging efficiency of adsorbents prepared from Raphia hookeri fruit waste, Sustain. Chem. Pharm. 12 (2018) 100141 December2019, doi:10.1016/j.scp.2019.100141.

[62] M.A. Ahmad, N. Ahmad, O.S. Bello, Adsorptive removal of malachite green dye using durian seed-based activated carbon, Water. Air. Soil Pollut. 225 (8) (2014), doi:10.1007/s11270-014-2057-z.

[63] P.N. Diagboya, B.I. Olu-Owolabi, K.O. Adebowale, Distribution and interactions of pentachlorophenol in soils: the roles of soil iron oxides and organic matter, J. Contam. Hydrol. 191 (2016) 99–106, doi:10.1016/j.jconhyd.2016.04.005.

[64] A. Oussalah, A. Boukerroui, A. Aichour, B. Djellouli, Cationic and anionic dyes removal by low-cost hybrid alginate/natural bentonite composite beads: adsorption and reusability studies, Int. J. Biol. Macromol. 124 (2019) 854–862, doi:10.1016/j.ijbiomac.2018.11.197.

[65] A.F. Lukman, K. Ayindez, Review and classifications of the ridge parameter estimation techniques, Hacettepe J. Math. Stat. 46 (5) (2017) 953–968, doi:10.15672/HJMS.201815671.

[66] A.F. Lukman, I. Dawoud, B.M.G. Kibria, Z.Y. Algamal, B. Aladeitan, A new ridge-type estimator for the gamma regression model, Scientifica (Cairo) 2021 (2021), doi:10.1155/2021/5545356.

[67] A.F. Lukman, B. Aladeitan, K. Ayinde, M.R. Abonazel, Modified ridge-type for the Poisson regression model: simulation and application, J. Appl. Stat. 49 (8) (2022) 2124–2136, doi:10.1080/02664763.2021.1889998.

[68] M. Qasim, K. Månsson, M. Amin, B.M. Golam Kibria, P. Sjölander, Biased adjusted poisson ridge estimators-method and application, Iran. J. Sci. Technol. Trans. A Sci. 44 (6) (2020) 1775–1789, doi:10.1007/s40995-020-00974-5.
[69] M. Qasim, B.M.G. Kibria, K. Månsson, P. Sjölander, A new Poisson Liu Regression Estimator: method and application, J. Appl. Stat. 47 (12) (2020) 2258–2271, doi:10.1080/02664763.2019.1707485.
[70] A.F. Lukman, E. Adewuyi, K. Månsson, B.M.G. Kibria, A new estimator for the multicollinear Poisson regression model: simulation and application, Sci. Rep. 11 (1) (2021), doi:10.1038/s41598-021-82582-w.
[71] A.E. Hoerl, R.W. Kennard, Ridge regression: biased estimation for nonorthogonal problems, Technometrics 12 (1) (1970) 55–67, doi:10.1080/00401706.1970.10488634.
[72] A.A. Inyinbor, F.A. Adekola, O.S. Bello, D.T. Bankole, T.A. Oreofe, A.F. Lukman, G.A. Olatunji, Surface functionalized plant residue in cu2+ scavenging: chemometrics of operational parameters for process economy validation, South African J. Chem. Eng. 40 (2022) 144–153 February, doi:10.1016/j.sajce.2022.03.001.
[73] M. Arashi, A.F. Lukman, Z.Y. Algamal, Liu regression after random forest for prediction and modeling in high dimension, J. Chemom. 36 (4) (2022), doi:10.1002/cem.3393.